

**Contributions of SLR for the Next Decade**  
**Thomas Herring,**  
**Massachusetts Institute of Technology, Cambridge, MA, USA**

**Abstract**

SLR is one of the corner stone geodetic methods that define today's modern geodetic infrastructure. The directions of geodetic science for the next decade will be defined by scientific problems to be addressed and the technology developments that allow the types of measurements needed to address these problems. One geodetic system will not be able to address all problems but the careful combination of the techniques available (VLBI, GNSS, DORIS and terrestrial measurements) is more likely to lead to advances. Here we examine where SLR is likely to fall in the mix of geodetic systems and in what directions should developments proceed for SLR to have maximum impact. We will re-visit issues related to range biases and how these impact correlations between atmospheric delays and height estimates, and the relationship between microwave technique and SLR sensitivities. Defining a geodetic reference system that allows global sea level to be determined with high spatial and temporal resolution while maintaining decade long stability will likely continue to be one of most stringent requirements for geodetic systems. We will carefully examine the scale difference between SLR and VLBI. Finally, we will look at the relative roles of SLR providing "service measurements" to other techniques and the science that can be done directly with SLR data.

**Introduction and scope**

We discuss here the contributions and challengers for SLR development and applications for the next decade. We will briefly review the types of errors that affect all geodetic measurement systems and how some of these errors might be addressed. We also examine "errors" in geodetic systems that represent deviations from linear motions that arise from the Earth itself and if correctly identified give us new insights into the deformation processes acting in the Earth. We then compare results from VLBI and SLR to assess the current state of the agreement between the systems. We conclude by looking at the challengers and opportunities for SLR in the next decade.

**Nature of geodetic noise signals**

Errors in geodetics systems can be divided into three main classes which we will refer to as instrumental, environmental, and Earth noises although the latter is more appropriately referred to as a signal. Instrumental noise can potentially be reduced to

arbitrarily small values with good (and often costly) engineering. Failure to understand instrument noise can lead to un-diagnosed errors. Environmental noise includes such items as propagation medium delays and satellite orbit perturbations. This class of noise can be modeled (atmospheric delay models), calibrated (e.g., dual frequency microwave systems), or estimated (atmospheric delay parameterization or empirical orbit model parameters). Better models and sources of data for the models and better parameterizations of models can be used to mitigate this class of error. In some cases, better observing strategies can also be used. For VLBI, strategies would include better, more rapid sky coverage. For GNSS, more channels to observe more satellites simultaneously and potentially including data from non-ground-based receivers are strategies that could be explored. For SLR, better satellite observation planning in terms of network coordinated observations of priority targets is a strategy that could be explored. Finally, Earth “noise” is a signal that we seek to explain but can be confused with possible instrumental or environmental noise i.e., treated as a noise source, or alternatively un-modeled instrumental or environmental noise could be interpreted as a deformation signal from the Earth. The separation of signal from noise in these cases depends on thorough understanding of the system noise and the ability to validate the signal through other data types or models.

Deformations arising from hydrological changes and so-called episodic tremor and slip (ETS) [Rogers and Dragert, 2003; Gomberg, 2010] are two examples of processes seen in geodetic time series that have been validated via models and other data sets such as GRACE for hydrology and seismic tremor for ETS events. A review by Bock and Melgar [2016] discusses many aspects of these classes of signals. Many of the studies of hydrology and ETS have used dense GPS/GNSS networks and other spatially dense systems such as Interferometric Synthetic Aperture Radar (InSAR) but similar types of processes will also affect sites in lower density VLBI and SLR networks. Dense networks around fundamental stations is one way of assessing the magnitudes of non-secular signals at VLBI and SLR stations.

### **Instrumental and environmental noise**

In the category of instrumental and environmental noise, we briefly explore multi-color ranging as an instrumental method of reducing atmospheric delay modeling error and we look at the impact of range biases.

#### *Atmospheric delay noise*

At optical frequencies, air is a dispersive medium with frequency dependencies for each of the major constituents of moist air. For most of the atmospheric constituents the mixing ratio is constant both in geographic location and altitude and thus one

composite refractive index formula can be generated. The two gas exceptions are carbon dioxide which is increasing with time and water vapor which is space and time dependent. The CO<sub>2</sub> effects have been discussed in *Ciddor* [1996] and can in principle be handled easily. Water vapor on the other hand is more problematic especially if instrumental multi-wavelength ranging is to be used to determine the total atmospheric delay. Multi-color laser ranging has been used successfully but care is needed in treating water vapor (see e.g., *Langbein et al.*, [1987]).

There are two possible approaches here. Dual color ranging will be sensitive to errors in modeling the water vapor delays. In Table 1, we give examples of dual frequencies combinations in near-infrared, green, and UV frequencies. In the table we show the impact of the total water vapor delay. In the dual color formulation, the range corrected for a dispersive delay is

$$R_c = F\lambda_1 R_1 + F\lambda_2 R_2 \quad (1)$$

where  $F\lambda_1$  and  $F\lambda_2$  are the factors multiplying the range measurements,  $R_1$  and  $R_2$ , using lasers with wavelengths  $\lambda_1$  and  $\lambda_2$ , and  $R_c$  is the range corrected for the refraction due to the dry constituents in the atmosphere. The *Owens* [1967] refractive index formulas were used to generate the table. The laboratory experiments for these formulas often date back to the 1930s well before the idea on mm-accuracy ranging to objects well outside the atmosphere were considered. The amplification of any noise in the range measurements can be seen in the magnitudes of the factors and any errors in the water vapor delay will also be amplified. By choosing shorter wavelength, the noise amplification can be reduced but the error due to water vapor is increased. Some caution should be exercised here because the UV wavelength is close to the wavelength limits used to derive the wavelength dependence.

**Table 1:** Sensitivity factors and impact of water vapor on the corrected ranges.

Wavelengths ( $\mu\text{m}$ )	$F\lambda_1$	$F\lambda_2$	Wet Delay* (mm)	Wet Error (mm)
1.024/0.512	20.7	-19.7	2.9	-7.9
0.512/0.256	5.0	-4.0	3.5	-20.8

\* The wet delay was computed for temperature 27C, 100% relative humidity. The corresponding micro-wave delay was 213 mm.

The water effect shown in Table 1 can be reduced by having a good calibration of the water vapor delay. The experience from micro-wave data processing is that apriori calibration of the water delay is typically only accurate to 50%. However, synergistic use of microwave and laser systems would be to use the microwave system estimates of the water vapor delay to determine an estimate of the optical frequency delay. The

complication here is that the microwave delay is dominated by the water vapor density over temperature while the optical delay depends only on density. Use of an a priori temperature profile and water vapor height distributions would probably suffice for the calibration because there a factor of 50-75 between the magnitudes of the two delays. Another approach is tri-wavelength ranging where the water vapor delay would be estimated. The corrected range factors for some choices of laser wavelengths are given in Table 2. The factors are larger than the dual wavelength systems but only by 2-3. However, it must be stressed that these factors will depend critically on the accuracy of the refractive index formulas.

**Table 2:** Tri-color laser ranging sensitivity. Range values at the three wavelengths would be combined with the factors given to generate a range estimates free from dry and wet refractivity contributions.

Wavelengths ( $\mu\text{m}$ )	$F\lambda_1$	$F\lambda_2$	$F\lambda_3$
1.024/0.512/0.256	33.43	-34.89	2.47
1.024/0.512/0.341	46.56	-59.72	14.16

#### *Range bias noise*

The impact of range biases arises from the correlations between range bias, station height and atmospheric delays. This correlation can be seen through the partial derivatives of a range bias being 1, the height estimate being  $-\sin \varepsilon$ , and the atmospheric delay being  $(\sim 1/\sin \varepsilon)$ , where  $\varepsilon$  is the elevation angle to the satellite of the observation. For high elevation angles,  $\varepsilon \sim \pi/2$ , all these partial derivatives are near unity and the deviation from 1 for the height and atmospheric delay goes as  $(\pi/2 - \varepsilon)^2$ . Simple behavioral characteristics can be assessed by simulating data uniformly spaced in elevation angle between zenith and a minimum elevation angle. For SLR ranging to LAGEOS, this minimum is often  $20^\circ$ . We illustrate the interaction of effects in Figure 1. This figure show a simulation of the error in the height estimate that results from a 10 mm error (nominal value, corresponding to  $\sim 4$  mbar pressure error) in the zenith atmospheric delay used in processing when range biases are held fixed and when they are estimated. For measurements restricted to near zenith, the +10 mm atmospheric delay error would make the estimate of the site 10 mm lower (i.e., the sum height error and atmospheric delay error would be near zero). The height error grows more negative as more lower elevation angle data are collected. The impact of the correlations of the parameters is that if a range bias is estimated, the height error changes sign and becomes a positive error. The sensitivity to the minimum elevation also increases as more lower elevation angle data are added.

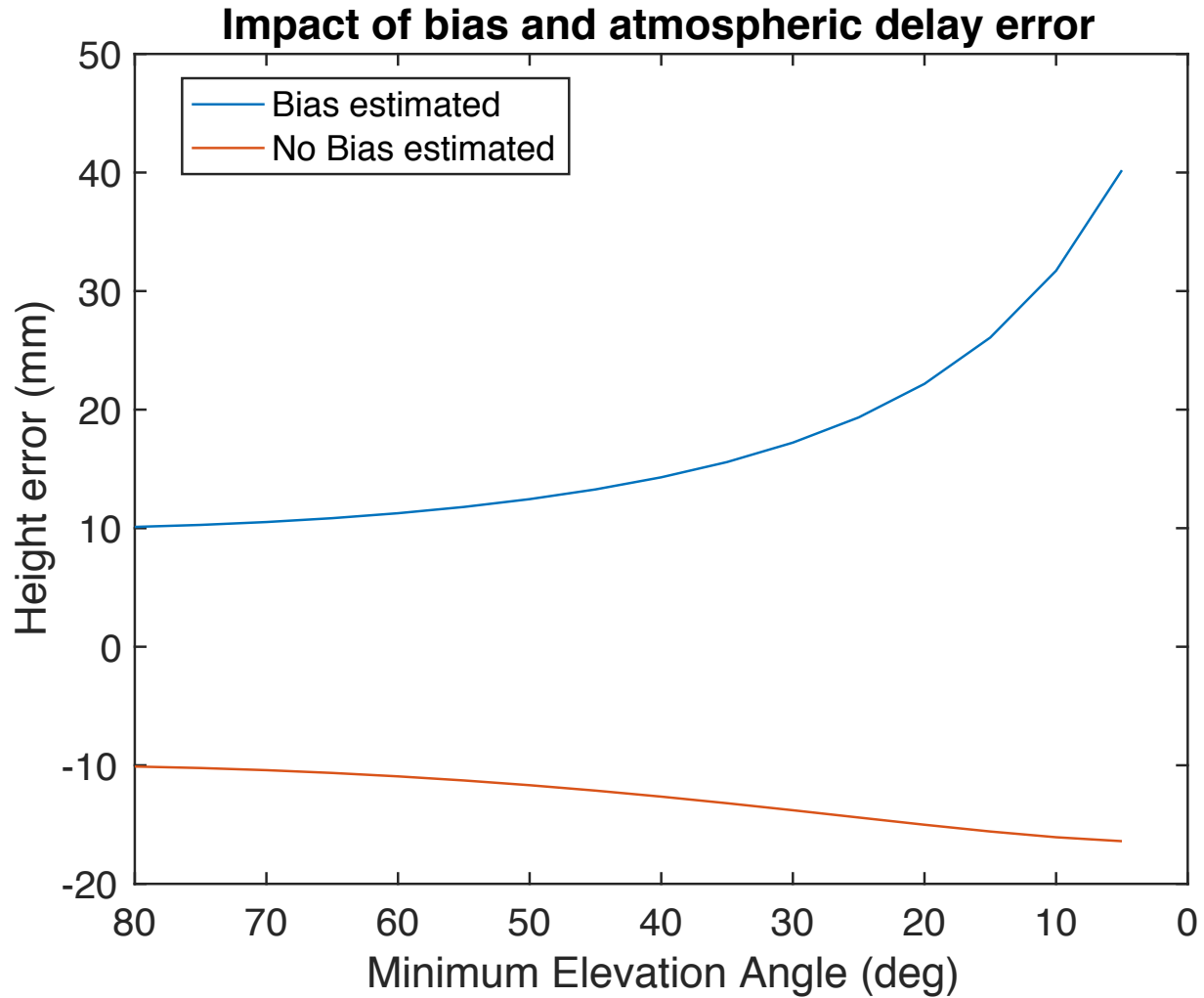


**Figure 1:** Example of the impact of a 10 mm atmospheric zenith delay error on height estimates with (blue line) and without (brown line) a range bias being estimated.

There are two conclusions to be drawn from this simple analysis (1) a systematic change in height estimates when range biases are estimated could arise from atmospheric delay modeling errors and not actual range biases and (2) The opposite signed effect on height estimates due to atmospheric delay errors between when bias estimated, which is always the case from microwave systems with independently running clocks, and no range bias estimates, which is the ideal processing method with SLR, could be exploited in combined microwave plus optical processing to reveal common atmospheric delay errors. The most serious limitation of the latter approach is that the atmospheric delay errors in microwave systems arises from the dipole component of water vapor refractive index which has little (no) effect optical ranging. However, with excellent engineering for the SLR systems to eliminate range biases and for measurement of

water vapor delays using radiometers for the microwave systems, the combined system could considerably reduce the impact on non-hydrostatic variations in atmospheric delays.

## Comparison of VLBI and SLR results

The International Earth Rotation Service (IERS) generates international terrestrial reference frame (ITRF) solutions by combining results from SLR, VLBI, GPS and DORIS. The latest realization is ITRF2014 [Altamimi *et al.*, 2016]. For the analysis of the differences between VLBI and SLR we examined the collocated sites that have survey ties between the VLBI and SLR systems. There are globally 25 VLBI/SLR sites in the ITRF2014 solution that are within 10 km of each other. Survey tie accuracy of sites separated by <10 km should be better than a few millimeters (0.1 parts-per-million is 1 mm). Not all these stations have large amounts of high quality data. If we restrict the pairs to those pairs where both the VLBI and SLR site have velocities in the ITRF2014 with standard deviations <1 mm/yr, we are left with 17 pairs. The very disappointing result is that only 6 of these pairs have survey ties between the VLBI and SLR sites.

For our analysis here we used the SLRa ITRF2014 combined SINEX files used in ITRF2014 (data ends 2015.0) and we used the on-going IVS combined SINEX files. These data in our analysis end in September 2018. We included all SINEX files for data collected after 1996 to be consistent the GPS time span available and to exclude earlier, lower quality results. We performed both time series analyses allowing rotation and translation of each SINEX file onto the ITRF2014 reference frame, and combined velocity estimate solutions where all the SINEX files for each system are combined separately into a single solution. The survey ties were applied to the VLBI solution to generate estimates of the SLR site positions. These estimates were compared to the SLR coordinates computed from the SLR SINEX files. The results of the comparison would be the same if we applied the survey ties to the SLR solution and compared to the VLBI estimates. A summary of the differences between the ITRF2014 and our estimates are given in Table 3. The epoch of our values is at the end of the data spans because of our use of a Kalman filter estimator in which the state vector always refers to the current time in the solution. Our scale difference shows VLBI estimates of height above those of SLR but the magnitude is about half that of the ITRF2014 estimate.

The standard deviations given in Table 3 are meant to represent realistic uncertainties of the estimates. In order to generate these standard deviations and to have the Kalman filter combine results with chi-squared-per-degree of freedom values near unity, we needed to scale both the SLR and VLBI covariance matrices by 50. If general users are to analyze results from the ILRS and IVS, care should be taken to make the covariance

matrices or normal equations in the SINEX have reasonable values and not to be so underestimated. Such underestimates can be confusing to users who expect covariances to reflect the statistical uncertainties in the parameter estimates given.

**Table 3:** Differences between height estimates at collocated VLBI and SLR sites with the ITRF2014 site tie vectors applied. The VLBI-SLR differences are a measure of the scale difference between VLBI and SLR. The mean difference excluding TIGO/CONZ is 3.9 mm corresponding to  $\sim 0.6$  ppb. (The VLBI estimate here is that of the SLR site generated by applying the site ties to the VLBI site coordinates).

Station	$\Delta U$ VLBI (mm)	$\Delta U$ SLR (mm)	VLBI-SLR (mm)
Wettzell	-11.9 $\pm$ 0.5	-13.0 $\pm$ 1.9	+1.1
Matera	-1.2 $\pm$ 0.6	-10.7 $\pm$ 0.8	+9.5
Yarragadee	8.0 $\pm$ 0.6	0.8 $\pm$ 0.7	+7.2
Hartebeesthoek	-2.9 $\pm$ 0.8	-3.2 $\pm$ 1.3	+0.3
McDonald, TX	-0.5 $\pm$ 0.8	-2.0 $\pm$ 0.9	+1.5
TIGO/CONZ	-11.5 $\pm$ 2.7	1.6 $\pm$ 2.1	-13.1

### Science with SLR

The science objectives for SLR can be divided into 6 main areas based in the ILRS web site (<https://ilrs.cddis.eosdis.nasa.gov/science/scienceContributions/index.html>)

1. The definition of the International Terrestrial Reference Frame (ITRF) by being the only space geodetic technique which (currently) defines the Earth's center of mass. In addition, SLR provides scale and the core network for the ITRF
2. Monitoring Earth rotation and polar motion to provide the relationship with The International Celestial Reference Frame (CRF)
3. Modelling the temporal and spatial variation of the Earth's gravity field
4. Determination of the Ocean and Earth tides
5. Monitoring tectonic plates and horizontal and vertical crustal deformation
6. Orbit determination for spaceborne altimeters and radar measurements for studies in global ocean circulation and changes in ice masses.

In each of these areas, other geodetic systems can also contribute and the boundaries between the different techniques and their contributions to different fields are fluid as technologies and analyses methods evolve. For example, monitoring Earth rotation in the presence of non-secular station motions needs a dense global network of sites which can be achieved with other less expensive systems such as GNSS networks. The precise contributions of individual methods will continue to evolve.

## **Conclusion: Science for the next decade:**

### *Challengers*

Developments in GNSS technologies and analysis method will certainly challenge SLR and other space geodetic system unique contributions. Specifically, the Galileo GNSS office has released far-field satellite transmission phase patterns for the Galileo satellites. The use of these patterns will remove the current uncertainty in GNSS scale and the results from the Galileo patterns can be transferred to other satellite systems such as GPS. With modern GPS satellites calibrated it will be possible to calibrate earlier GPS satellites and therefore the determination of terrestrial scale from GPS and GNSS for the whole GPS period should be possible. The next GPS/GNSS reprocessing to start in June 2019 will explore whether this approach will be successful.

The other challenge from GPS and GNSS will come from the release of satellite meta-data for Galileo satellites which should allow direct modeling of the radiation forces on these satellites (such as already in done for many scientific low earth orbiting satellites). With accurate direct modeling of the radiation forces there will be little or no need for empirical once-per-revolution parameters which directly affect the determination of the position of the center of mass relative to center of network. Also the globally dense GNSS networks can indirectly determine center of mass motions through the deformation field created by a degree-1 loading signal. If center of mass motions are due solely to masses that load the surface, then this approach becomes an independent method determining center of mass motions [Blewitt *et al.*, 2001; Blewitt, 2003; Wu *et al.*, 2003].

The SLR tracking of satellites is critical and becoming more commonly requested. The ILRS community will need to decide how to balance the “service role” of tracking many different satellites with achieving its own science directly. On-the-other hand, many of these other vehicles that are tracked could be used to improve geodetic results (especially the GNSS satellites which have extensive GNSS tracking as well).

### *Opportunities*

Optical un-biased range measurements are capable of much higher accuracies than GNSS phase measurements and the ILRS needs to exploit this. The bias in scale between VLBI and SLR could potentially be related to our atmospheric refractivity formulas. Did the original measurements consider the accuracy requirements of un-biased range measurements to objects well above the surface of the Earth and outside its

atmosphere? Can we exploit the difference in water vapor contributions to microwave and optical systems to better calibrate the atmospheric delays of both systems?

Understanding the motions of the center of mass of the Earth relative to center of figure using both dense GNSS data and sparse SLR data could lead to improved insights into the fluid motions around the Earth. A combined analysis where the loading effects on motions of stations can be used to both infer the degree-1 loading and thus center of mass shifts and a network shift approach (i.e., degree-1 terms in the gravity field) could be illustrative for mass motions that do not load the surface (e.g., fluid core motions at annual and longer time scales) or for transient deformation processes that are not loading (e.g., poro-elastic effects in aquifers). These types of analyses will require careful and consistent combinations of results from different space geodetic systems. Possibly, the Green's functions used to model the deformations from a loading source may be refined with these combinations.

One interesting area to consider is the impact of mass market laser ranging systems being developed for autonomous vehicle navigation and other LIDAR applications. Could these developments be exploited in the same way scientific GNSS applications benefit from cost-reductions due to the economy of scale manufacturing for consumer market.

As a final note, GNSS research has benefited greatly from the open availability of higher level products such as position time series, velocity fields and Earth orientation parameters that can be widely used and studied by the community. Ideally, these higher level products would have realistic standard deviations for the estimates. With temporally correlated noise, these realistic sigmas can be difficult to represent. For the ILRS, it should be possible for users to easily access center of mass motions, scale changes, time series and other geodetic products. Many different analyses of these results will lead to new discoveries and improvements to the analyses of SLR data which will benefit the whole Earth science community.

## References

- Altamimi, Z., P. Rebischung, L. Métivier, and X. Collilieux. 2016. "ITRF2014: A New Release of the International Terrestrial Reference Frame Modeling Nonlinear Station Motions." *Journal of Geophysical Research: Solid Earth* 121 (8). Wiley-Blackwell: 6109–31. doi:10.1002/2016JB013098.
- Blewitt, G., D. Lavallée, P. Clarke, and K. Nurutdinov. 2001. "A New Global Mode of Earth Deformation: Seasonal Cycle Detected." *Science* 294 (5550). <http://science.sciencemag.org/content/294/5550/2342>.

- Blewitt, G.. 2003. "Self-Consistency in Reference Frames, Geocenter Definition, and Surface Loading of the Solid Earth." *Journal of Geophysical Research: Solid Earth* 108 (B2). John Wiley & Sons, Ltd. doi:10.1029/2002JB002082.
- Bock, Yehuda, and Diego Melgar. 2016. "Physical Applications of GPS Geodesy: A Review." *Reports on Progress in Physics* 79 (10). doi:10.1088/0034-4885/79/10/106801.
- Ciddor, Philip E. 1996. "Refractive Index of Air: New Equations for the Visible and near Infrared." *Applied Optics* 35 (9). Optical Society of America: 1566–73. doi:10.1364/AO.35.001566.
- Gomberg, Joan. 2010. "Slow-Slip Phenomena in Cascadia from 2007 and beyond: A Review." *Geological Society of America Bulletin* 122 (7–8). GeoScienceWorld: 963–78. doi:10.1130/B30287.1.
- Langbein, J. O., M. F. Linker, A. F. McGarr, and L. E. Slater. 1987. "Precision of Two-Color Geodimeter Measurements: Results from 15 Months of Observations." *Journal of Geophysical Research: Solid Earth* 92 (B11). John Wiley & Sons, Ltd: 11644–56. doi:10.1029/JB092iB11p11644.
- Owens, James C. 1967. "Optical Refractive Index of Air: Dependence on Pressure, Temperature and Composition." *Applied Optics* 6 (1). Optical Society of America: 51. doi:10.1364/AO.6.000051.
- Rogers, Garry, and Herb Dragert. 2003. "Episodic Tremor and Slip on the Cascadia Subduction Zone: The Chatter of Silent Slip." *Science (New York, N.Y.)* 300 (5627). American Association for the Advancement of Science: 1942–43. doi:10.1126/science.1084783.
- Wu, X., M. B. Heflin, E. R. Ivins, D. F. Argus, and F. H. Webb. 2003. "Large-Scale Global Surface Mass Variations Inferred from GPS Measurements of Load-Induced Deformation." *Geophysical Research Letters* 30 (14). John Wiley & Sons, Ltd. doi:10.1029/2003GL017546.